SUPPORTING INFORMATION

Estimation of the Apparent Anisotropic Water Diffusivity on Spruce Evaluated with a Simplified Derivative Approach and as a Function of the Flow Rate

Antoni Sánchez-Ferrer[1,*], Max Engelhardt[1]

[1] Wood Materials Science, Wood Research Institute of Munich (HFM), TUM School of Engineering and Design, Technical University of Munich, Winzererstr. 45, 80797 Munich, Germany

Antoni Sánchez-Ferrer*: orcid.org/0000-0002-1041-0324; email: sanchez@hfm.tum.de

Max Engelhardt: orcid.org/0000-0002-9781-7476; email: engelhardt@hfm.tum.de

Appendix SI-A: The derivative method

In this appendix, the description of this derivative method (DER) for the calculation of the lifetime τ and the shape factor β is explained in detail. A series of simulated curves based on the single-stretched exponential function (SSE) or Weibull equation (Eq. SI-A1) are shown by varying the lifetime τ or the shape factor β to validate the DER method.

$$Y = 1 - e^{-\left(\frac{X}{\tau}\right)^{\beta}} \qquad \text{(Eq. SI-A1)}$$

Once the SSE curves are simulated (Fig. SI-A1a and SI-A2a) and as already mentioned in the Materials and Methods chapter (see "Derivative method for the determination of the apparent diffusion coefficient"), the steps for the DER procedure are the following:

1) Calculate the logarithm of all X values and plot Y *vs.* log X to obtain the corresponding S-shape curves (Fig. SI-A1b and SI-A2b);
2) Calculate the corresponding derivative dY/d(log X), which results on a peak function (Fig. SI-A1c and SI-A2c);
3) Normalize the dY/d(log X) *vs.* log X curve from 0 to 1 (Fig. SI-A1d and SI-A2d);
4) Localize the log X value corresponding to the maximum in the curve $dY/d(\log X)_{norm}$ *vs.* log X;
5) Calculate the FWHM by measuring the distance between the two points, one to the left and one to the right of the local maximum, that satisfy $dY/d(\log X)_{norm} = 0.5$.

In Fig. SI-A1, several SSE curves were simulated by varying the lifetime τ from 50 (red curve) to 150 (blue curve) in 10-unit steps and keeping the shape factor constant (β = 1). After transforming the abscissa values X to the corresponding log X values, all S-shaped curves were derived and normalized, and the corresponding peak function was obtained. The peak maximum is shifted when the τ value varies. Notice that the peak maximum at log t_{max} corresponds to the log τ value; therefore, the lifetime of a set of experimental data can be obtained by calculating the corresponding $t_{0.63}$ – the time at which the Y value is equal to 0.6321 – or by detecting the peak maximum in the derivative curve. After normalizing the derivative curves, the FWHM of each peak remains constant because the shape factor β is constant too.

In Fig. SI-A2, several SSE curves were simulated by varying the shape factor β from 0.6 (red curve) to 1.1 (blue curve) in 0.05-unit steps and keeping the lifetime constant (τ = 100). After transforming the abscissa values X to the corresponding log X values, all S-shaped curves were derived and normalized, and the corresponding peak function was obtained. Notice that the peak maximum of all curves is at log $t_{max,}$ which corresponds to the constant value of log τ = 2. The FWHM values – the distance between the two points at dY/dX_{norm} = 0.5 to the left and to the right of the peak maximum – are inversely proportional to the shape factor, *i.e.*, the smaller the β values, the larger the FWHM, and vice versa.

In order to find out the relationship between the FWHM of the peak function and the shape factor β from the SSE curve, a power law fitting was conducted, showing a reciprocal correlation between the two parameters, *i.e.*, FWHM = 1.06227 β^{-1} (Fig. SI-A3). Therefore, from the analysis of the FWHM in the derivative curve, the shape factor β of the corresponding SSE curve can be evaluated.

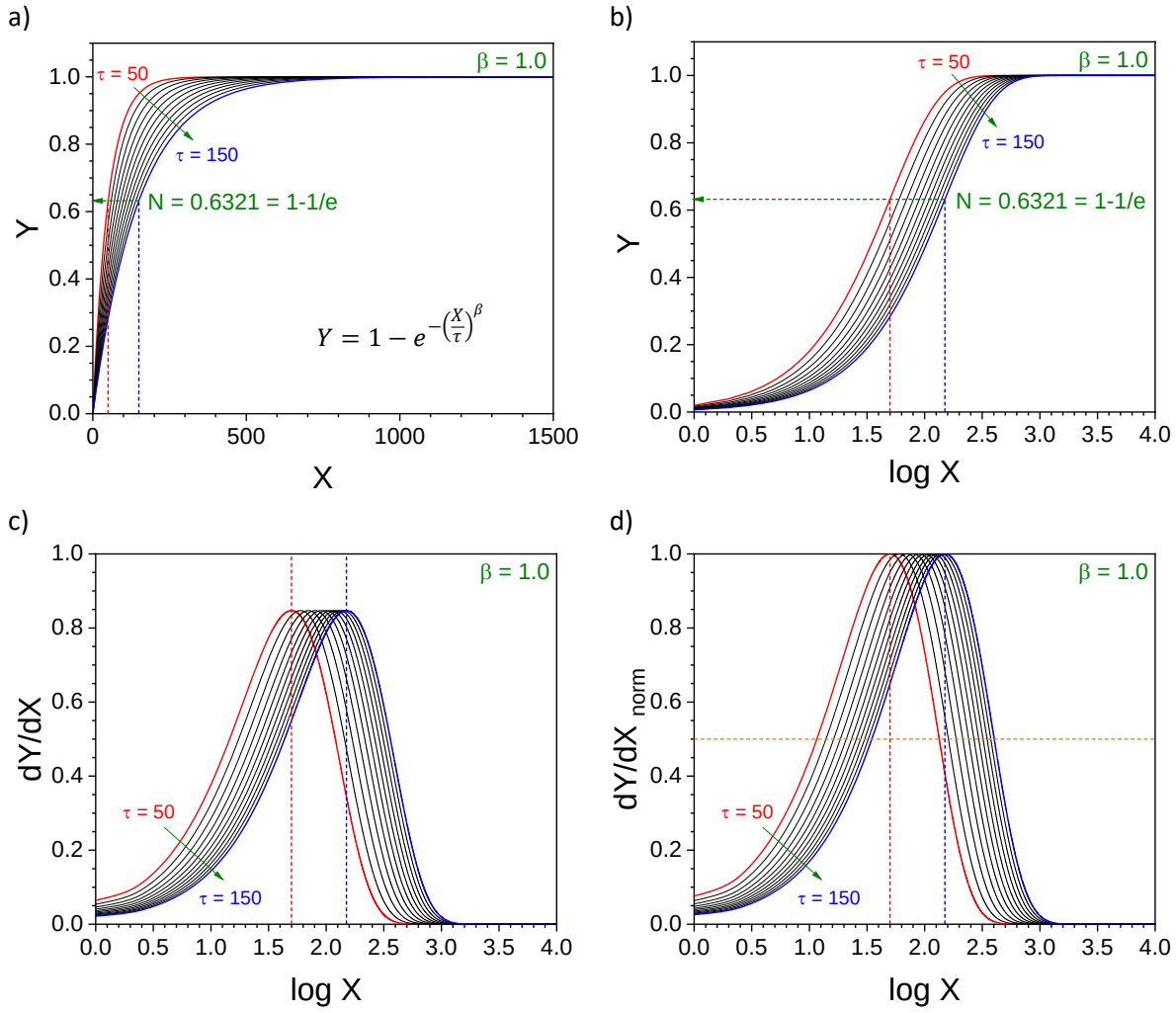

Fig. SI-A1. a) Simulated SSE curves varying the lifetime τ from 50 (red curve) to 150 (blue curve) and keeping the shape factor constant (β = 1). b) S-shape simulated SSE curves after transforming the abscissa values from X to log X. c) Derivative curves showing a shift in the peak maximum as a function of the lifetime τ and constant FWHM. d) Normalized derivative curves. Note: the lifetime value τ corresponds to the time at which the Y values equal 1-1/e ≈ 0.6321 = 63.21%.

Finally, in order to verify the independence between the two SSE parameters, *i.e.*, τ and β, three sets of curves were simulated with values of τ = 50, 100 and 150 and varying the shape factor β between 0.6 and 1.1 (Fig. SI-A4). The results show that the peak maximum is directly proportional to the lifetime τ value, and the FWHM is inversely proportional to the shape factor β no matter of the τ value. Therefore, both parameters can be evaluated from the derivative independently.

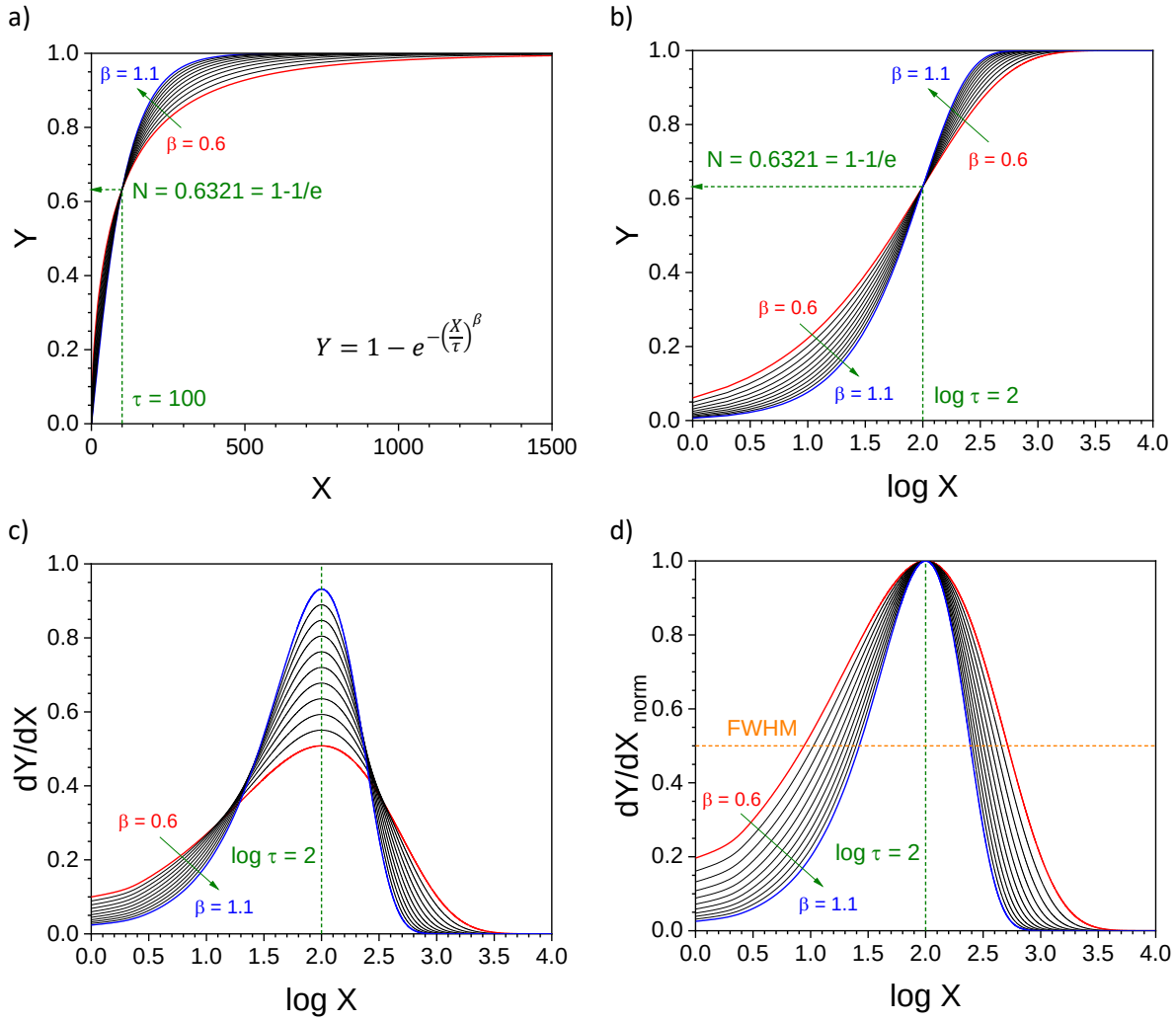

Fig. SI-A2. a) Simulated SSE curves varying the shape factor β from 0.6 (red curve) to 1.1 (blue curve) and keeping the lifetime t constant (τ = 100). b) S-shape simulated SSE curves after transforming the abscissa values from X to log X. c) Derivative curves showing a change in the peak width as a function of the shape factor β and constant peak maximum log t_{max}. d) Normalized derivative curves. Note: the lifetime value τ corresponds to the time at which the Y values equal 1-1/e ≈ 0.6321 = 63.21%.

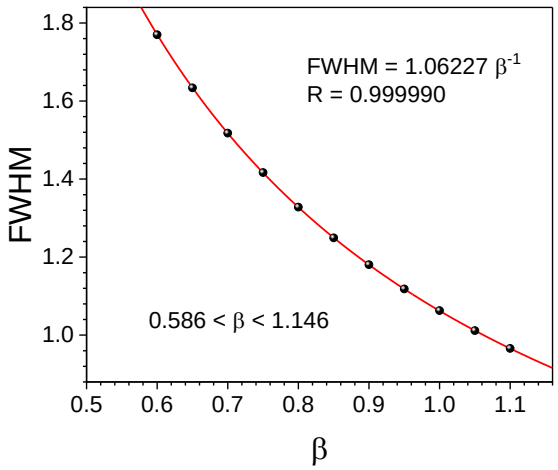

Fig. SI-A3. Reciprocal correlation between the FWHM of the normalized derivatives and the shape factor β values between 0.586 < β < 1.146. Note: data were obtained from Fig. SI-A2d.

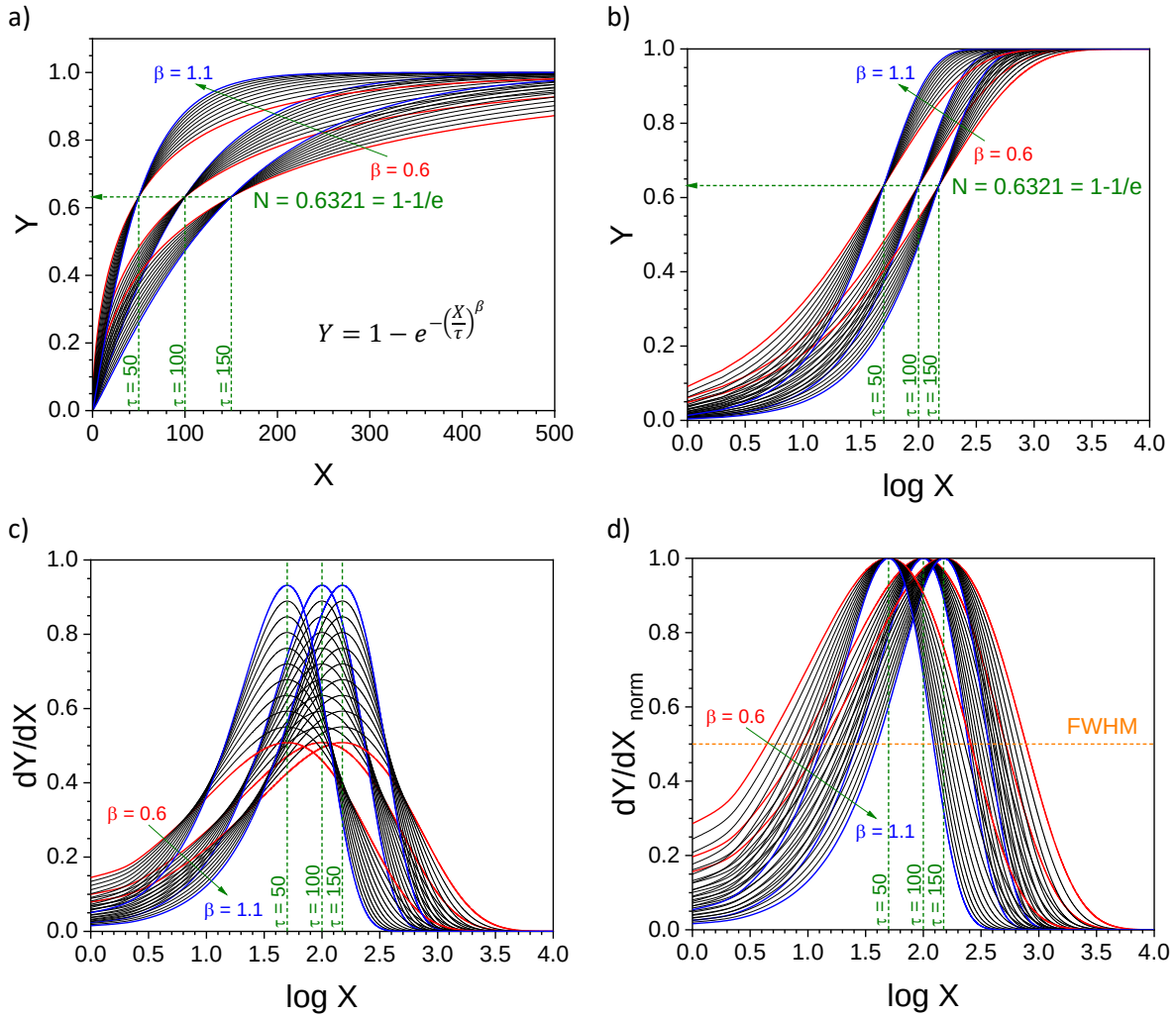

Fig. SI-A4. a) Three sets of simulated SSE curves with lifetime t values of 50, 100 and 150 and with shape factor β values from 0.6 (red curve) to 1.1 (blue curve) for each set. b) S-shape simulated SSE curves after transforming the abscissa values from X to log X. c) Derivative curves showing a shift in the peak maximum as a function of the lifetime τ and a change in the peak width as a function of the shape factor β. d) Normalized derivative curves. Note: the lifetime value τ corresponds to the time at which the Y values equal 1-1/e ≈ 0.6321 = 63.21%.

The advantages of this method are that the plateau in the mass uptake during the sorption process does not have to be reached, as soon as the peak maximum in the derivative t_{max} is achieved. Therefore, implementing a numerical protocol following the DER method during the signal monitoring can detect such a $t_{max} \approx \tau_1$., and the corresponding apparent diffusion coefficient can be easily calculated. Moreover, from the analysis of the peak's FWHM, the shape factor β can be calculated, and the diffusion process can be classified, *e.g.*, as a Fickian or non-Fickian process. Finally, there is no need to conduct any fitting procedure or apply any model.

Appendix SI-B: The Gumbel density function

In this appendix, the linkage between the single-stretched exponential function (SSE) and the Gumbel density function (GDF) is described. The GDF is a case of the Generalized Extreme Value (GEV) distribution with a peak function or probability density function (PDF) indicated in Eq. SI-B1,

$$Y = Ae^{-e^{-\left(\frac{\rho-X}{\omega}\right)}-\frac{\rho-X}{\omega}+1} \qquad \text{(Eg. SI-B1)}$$

where A is the amplitude, ρ is the peak maximum, and ω is the scale parameter.

A series of single-stretched exponential (SSE) functions was simulated by varying the shape factor β from 0.60 to 1.10 and keeping the lifetime constant τ = 100, which corresponds to the data in Fig. SI-A2b. The DER method was applied in order to obtain the corresponding peak distribution curves and fitted with the GDF (Fig. SI-B1). The fitting results show a perfect correlation between the lifetime τ and the peak value ρ, *i.e.*, $\tau = 10^{\rho}$ or $\rho = \log \tau$.

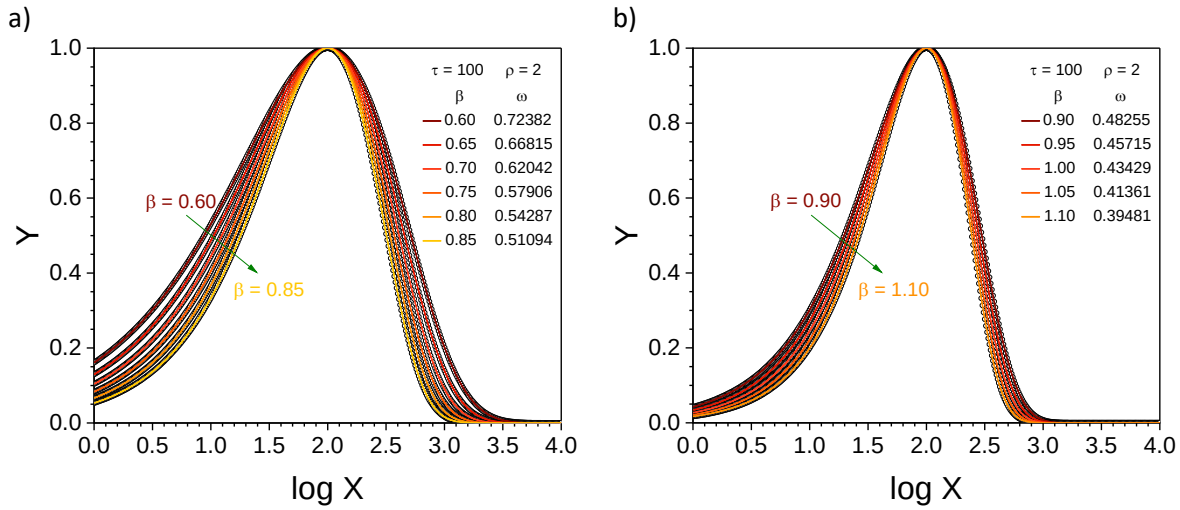

Fig. SI-B1. Simulated SSE functions (empty symbols) - τ = 100 and 0.60 < β < 1.10 - and the corresponding GDF fitting curves (colored curves) - ρ =2 and 0.72382 < ω < 0.39481. a) 0.60 < β < 0.85 and b) 0.90 < β < 1.10.

Moreover, the mathematical relationship between the shape factor β from the SSE function and the scale parameter ω from the GDF was found to be reciprocal or a power law with an exponent value of n = -1 (Fig. SI-B2), *i.e.*, $\omega = 0.434295\ \beta^{-1}$.

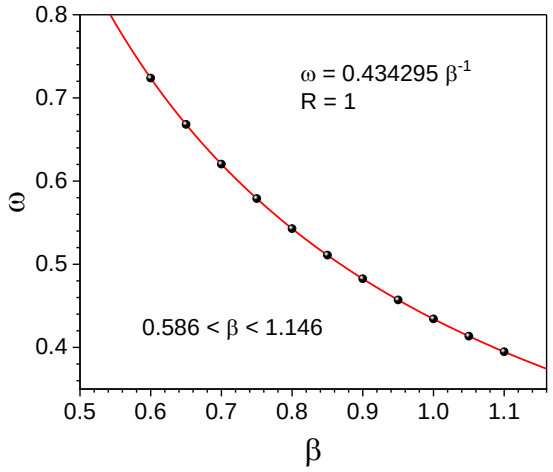

Fig. SI-B2. Reciprocal correlation between the scale parameter ω (GDF) and the shape factor β (SSE).

Finally, because all DVS data were adjusted with a DSE function, some series of double-stretched exponential (DSSE) functions were simulated by keeping constant the fast sorption process ($\tau_1 = 10$) and varying the slow sorption process ($50 < \tau_2 < 1000$) with different shape factor values β_1 and β_2. As before, the DER method was applied, the corresponding peak distribution curves were obtained and fitted with a double-Gumbel density function (DGDF) (Fig. SI-B3, SI-B4 and SI-B5). In this way, the effect on the τ_2, β_1 and β_2 values on the peak maximum t_{max} was evaluated, and the shift percentage with respect to the τ_1 was calculated for each case (Fig. SI-B6). The results show that the maximum shift between the peak maximum in the total curve t_{max}, and the peak maximum of the fast sorption process τ_1 is below 10%. Therefore, when the lifetime of the slow sorption process is far larger than that of the fast sorption process, one can assume $t_{max} \approx \tau_1$ by only localizing the peak maximum from the experimental DVS data.

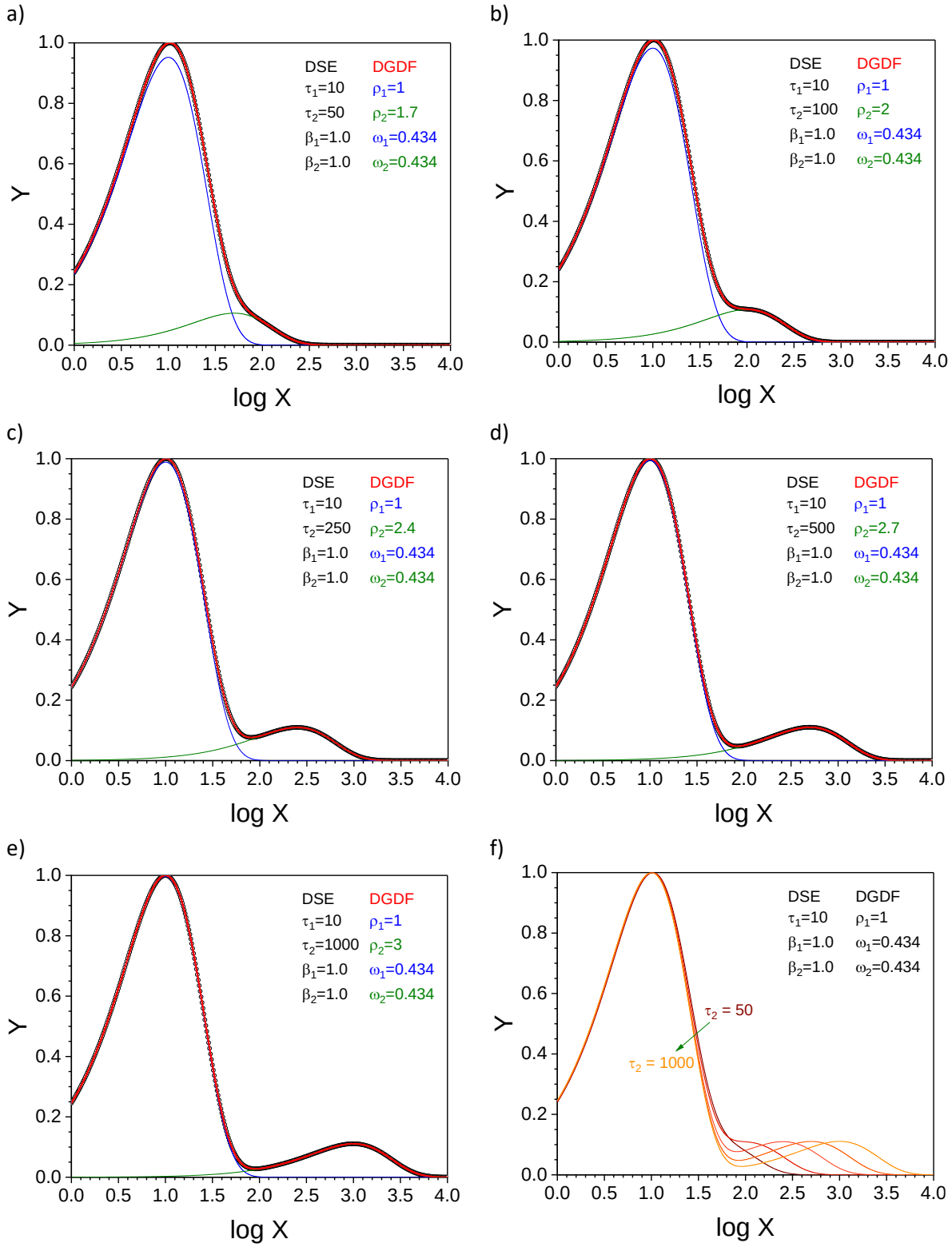

Fig. SI-B3. Series of simulated DSE curves (empty symbols) - τ_1 = 10, β_1 = 1.0, β_2 = 1.0, and τ_2 = a) 50, b) 100, c) 250, d) 500, and e) 1000 - and the corresponding double GDF (DGDF) fitting curves (red). F) DGDF fitting curves for the different τ_2 values, *i.e.*, 50, 100, 250, 500 and 1000.

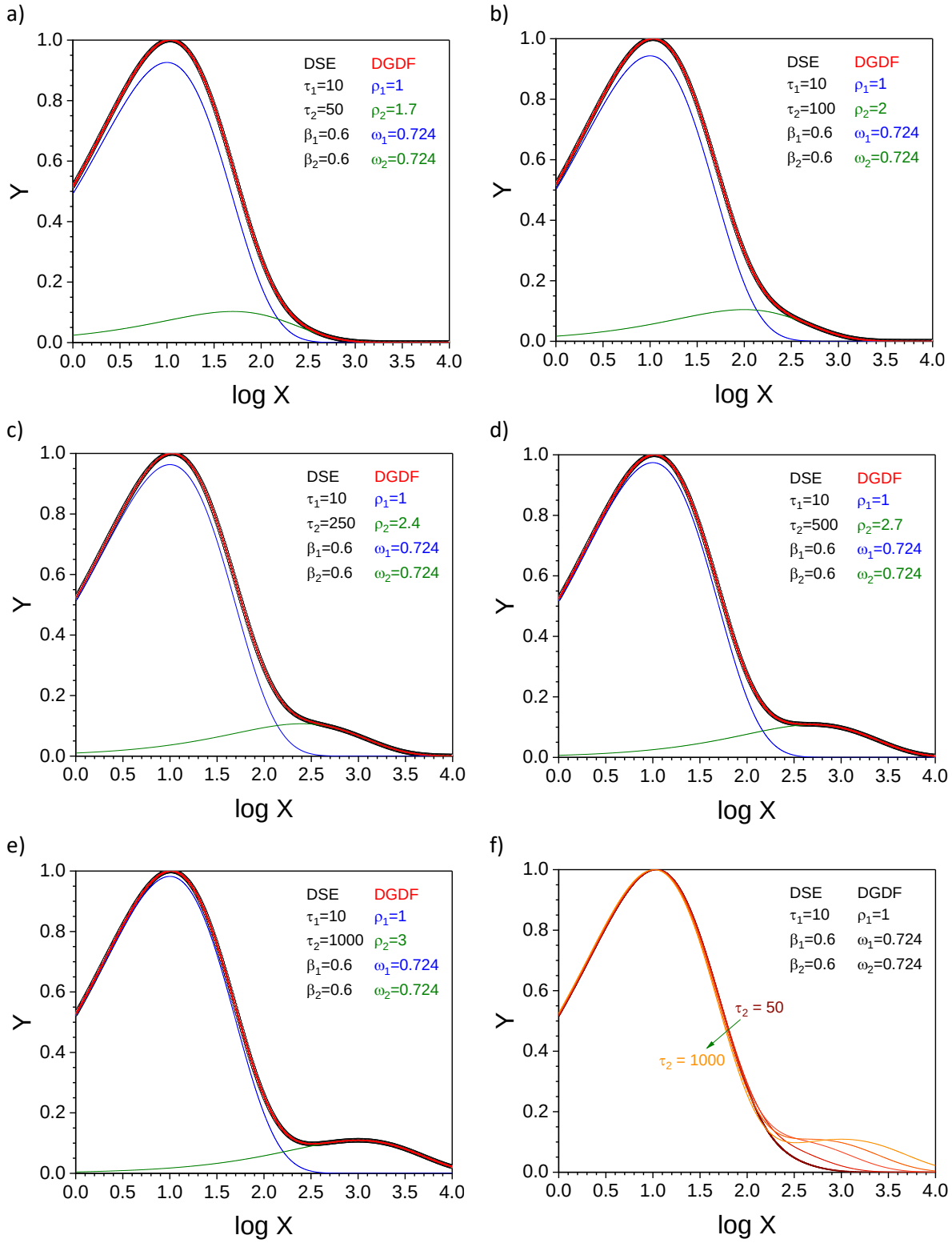

Fig. SI-B4. Series of simulated DSE curves (empty symbols) - τ_1 = 10, β_1 = 0.6, β_2 = 0.6, and τ_2 = a) 50, b) 100, c) 250, d) 500, and e) 1000 - and the corresponding double GDF (DGDF) fitting curves (red). F) DGDF fitting curves for the different τ_2 values, *i.e.*, 50, 100, 250, 500 and 1000.

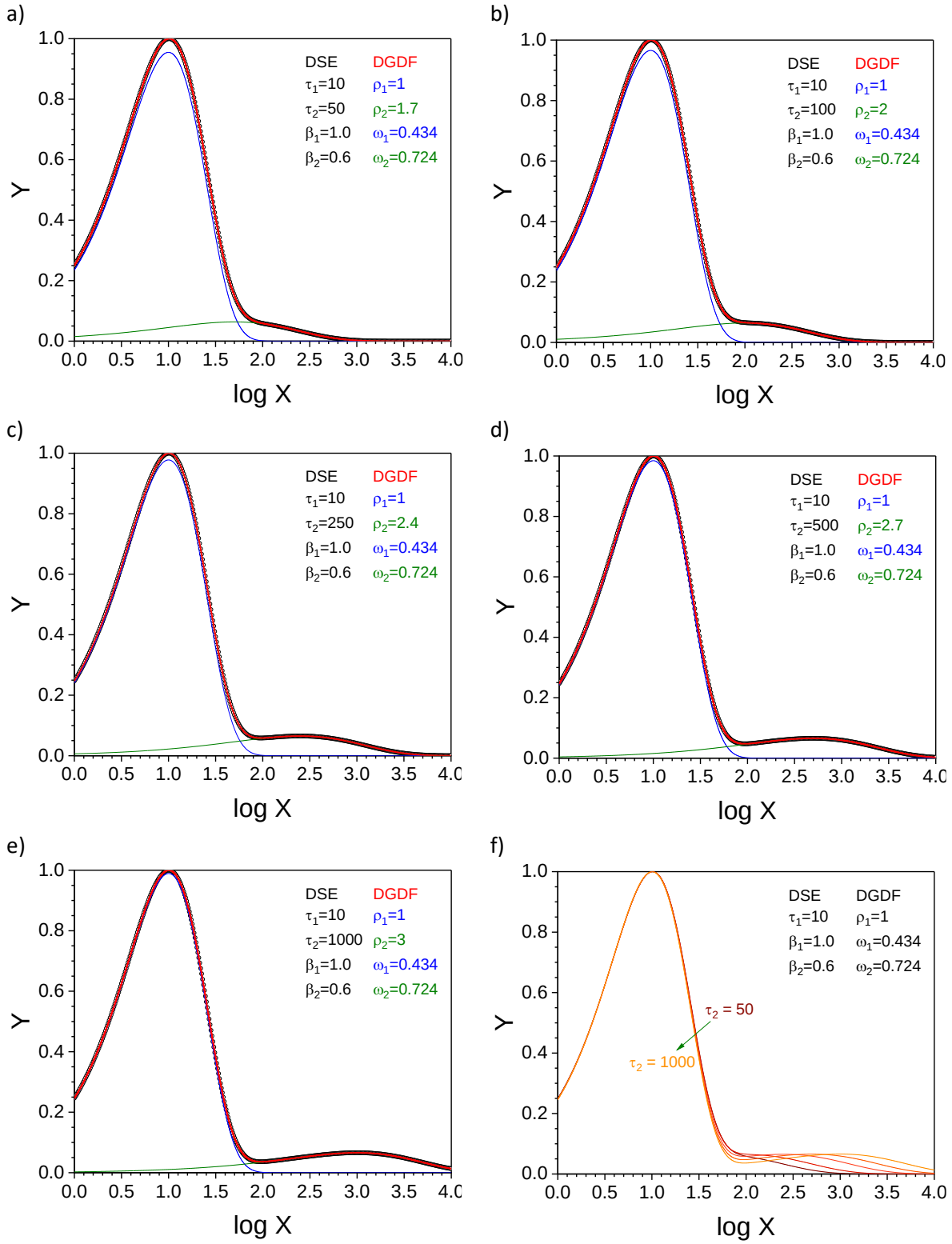

Fig. SI-B5. Series of simulated DSE curves (empty symbols) - τ_1 = 10, β_1 = 1.0, β_2 = 0.6, and τ_2 = a) 50, b) 100, c) 250, d) 500, and e) 1000 - and the corresponding double GDF (DGDF) fitting curves (red). F) DGDF fitting curves for the different τ_2 values, *i.e.*, 50, 100, 250, 500 and 1000.

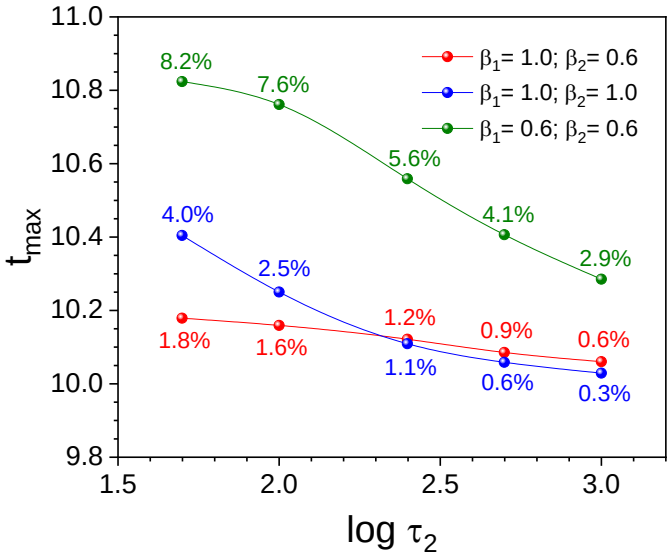

Fig. SI-B6. Peak maximum t_{max} - from the fitting of the simulated DSE function with a DGDF - as a function of the slow process lifetime τ_2 with the constant value τ_1 = 10, and for different shape factor values β_1 and β_2.

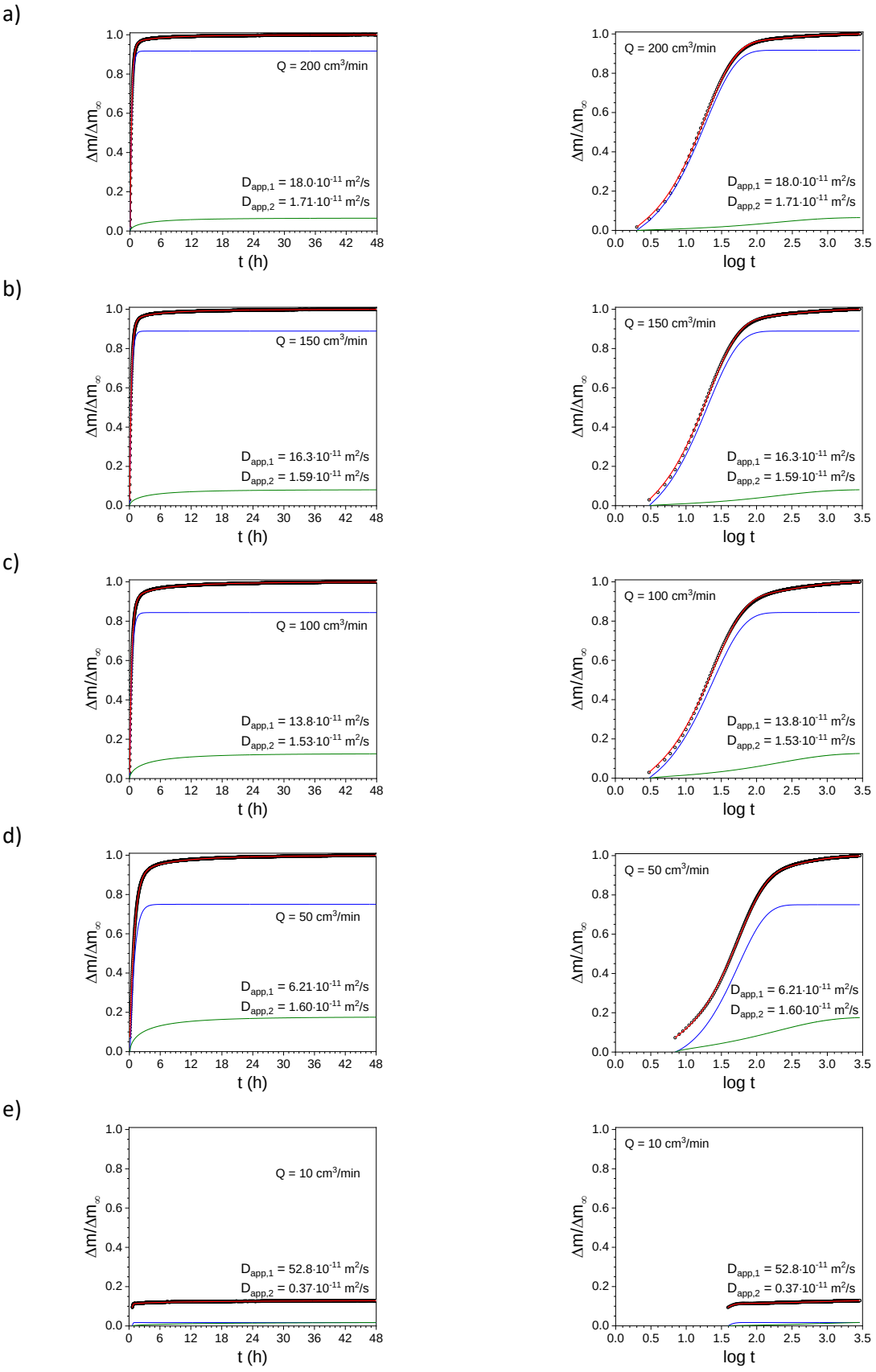

Fig. SI-1. lin-lin (left column) and lin-log (right column) plots of the time-sorption isotherm DVS data at different flow rate values Q for the spruce disk in the **L-direction**, together with the corresponding **DSE** fitting curve.

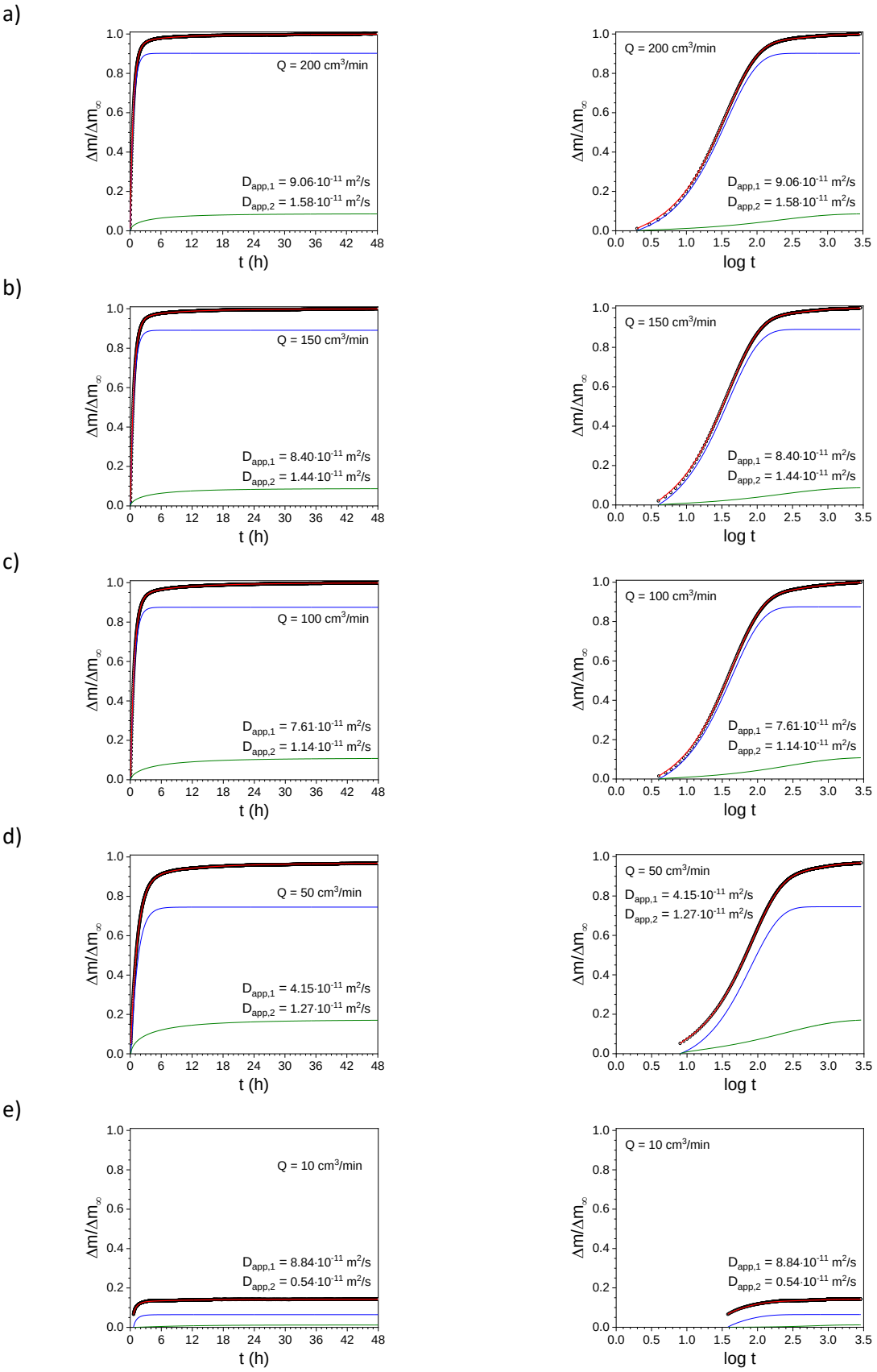

Fig. SI-2. lin-lin (left column) and lin-log (right column) plots of the time-sorption isotherm DVS data at different flow rate values Q for the spruce disk in the **R-direction**, together with the corresponding **DSE** fitting curve.

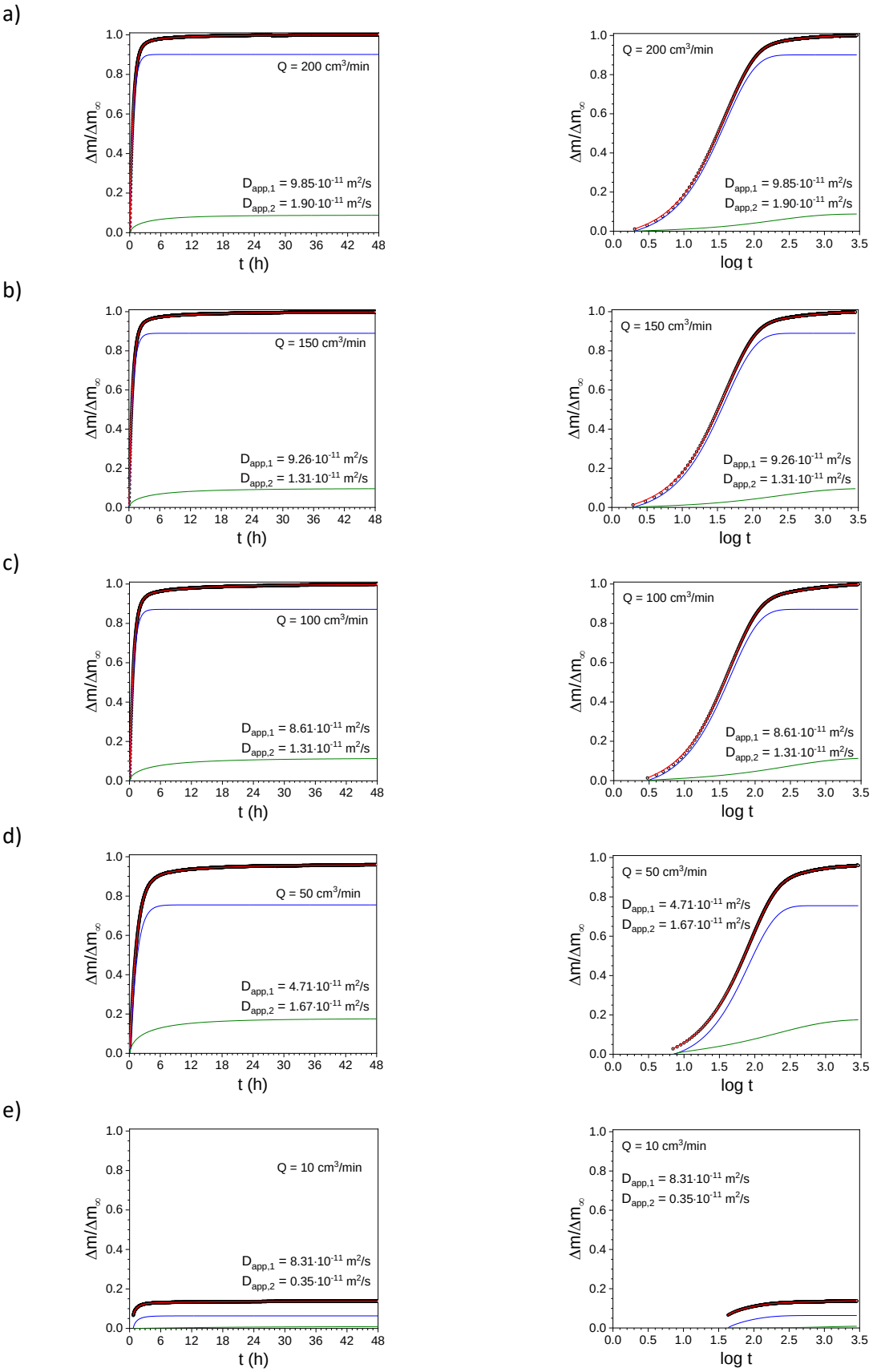

Fig. SI-3. lin-lin (left column) and lin-log (right column) plots of the time-sorption isotherm DVS data at different flow rate values Q for the spruce disk in the **T-direction**, together with the corresponding **DSE** fitting curve.

a)

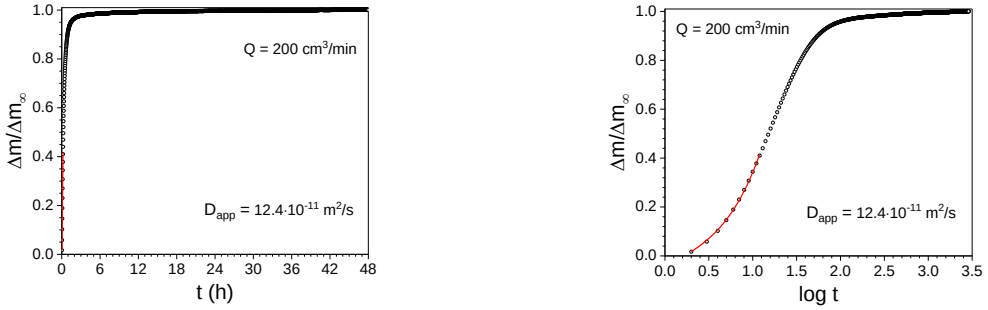

b)

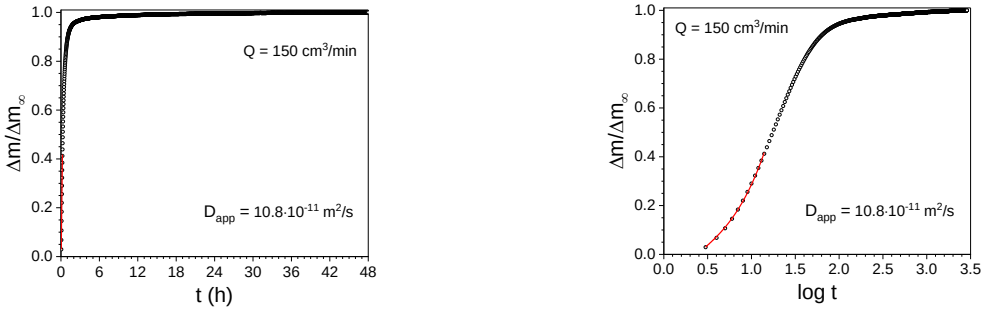

c)

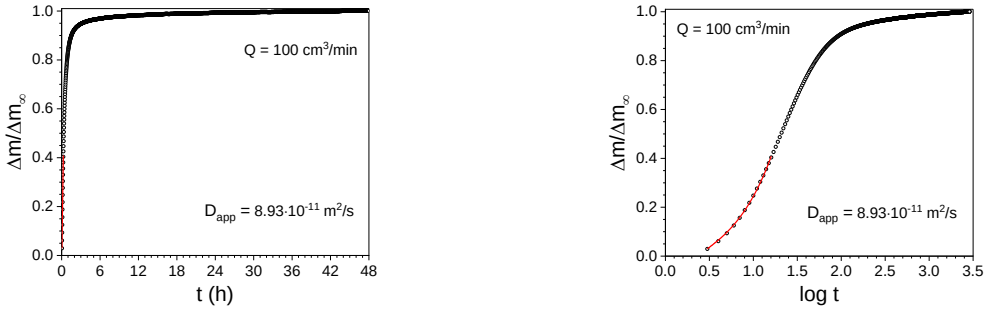

d)

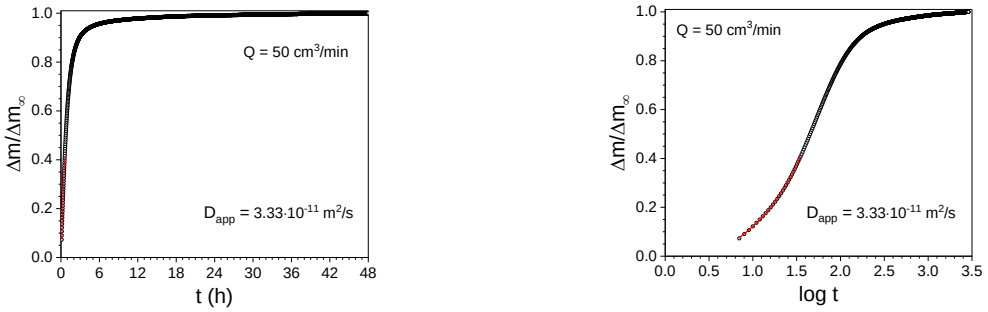

Fig. SI-4. lin-lin (left column) and lin-log (right column) plots of the time-sorption isotherm DVS data at different flow rate values Q for the spruce disk in the **L-direction**, together with the corresponding **RP** fitting curve.

a)

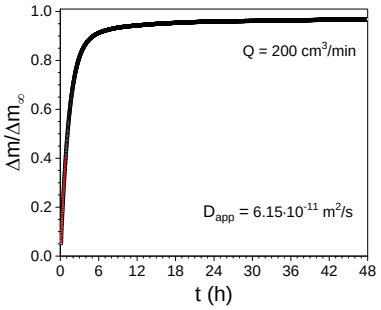

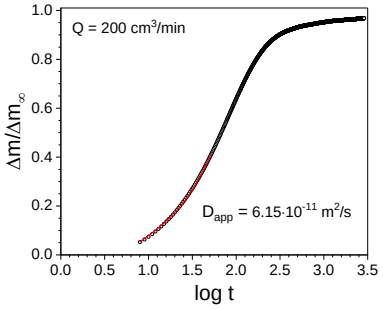

b)

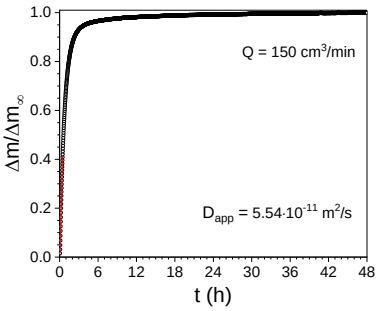

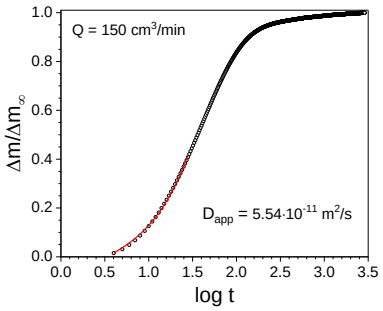

c)

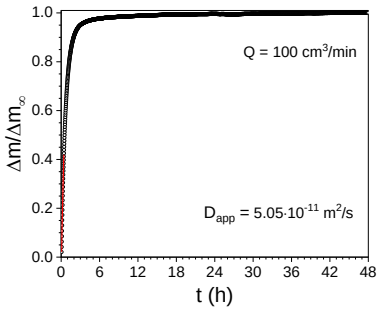

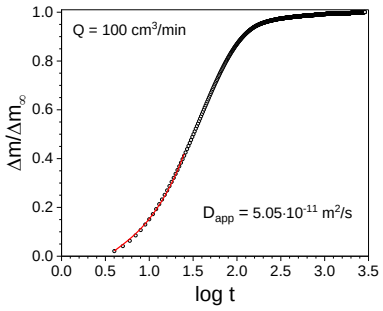

d)

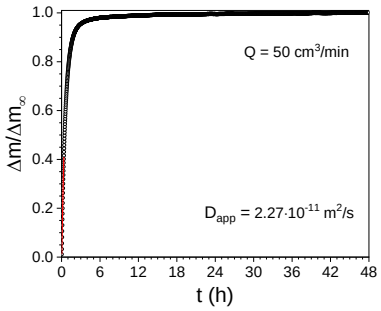

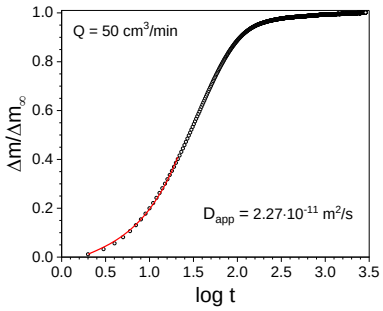

Fig. SI-5. lin-lin (left column) and lin-log (right column) plots of the time-sorption isotherm DVS data at different flow rate values Q for the spruce disk in the **R-direction**, together with the corresponding **RP** fitting curve.

a)

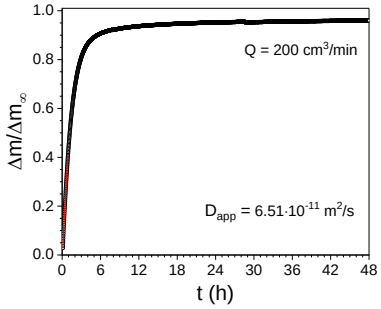

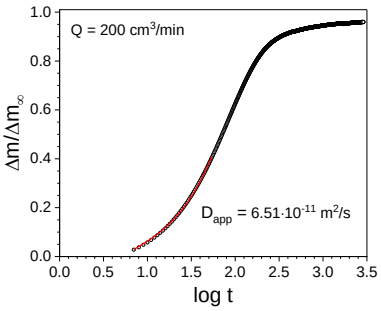

b)

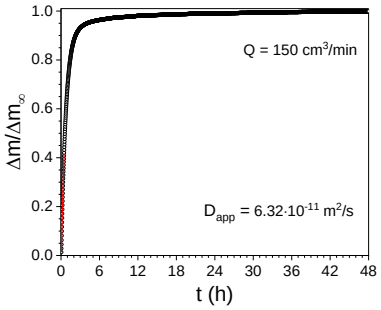

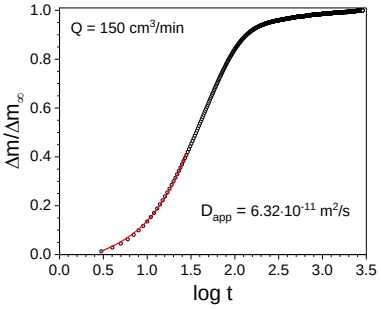

c)

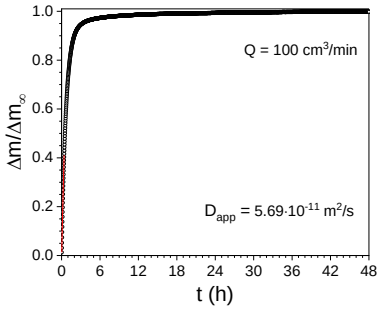

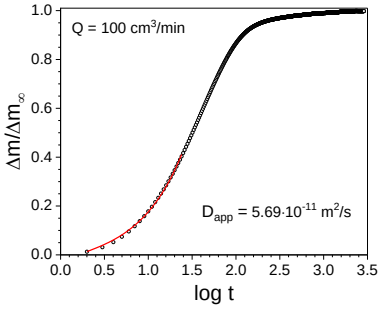

d)

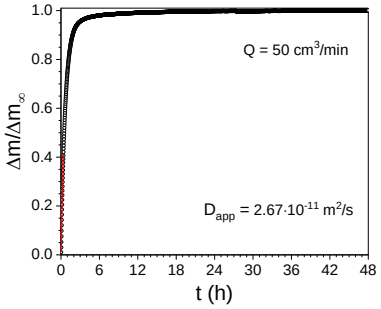

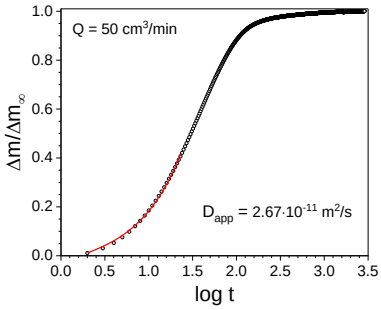

Fig. SI-6. lin-lin (left column) and lin-log (right column) plots of the time-sorption isotherm DVS data at different flow rate values Q for the spruce disk in the **T-direction**, together with the corresponding **RP** fitting curve.

a)

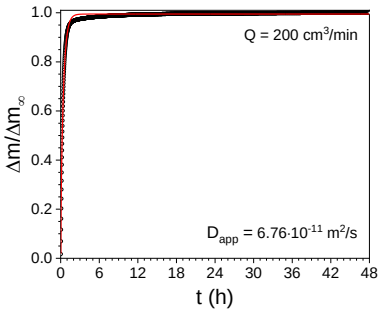

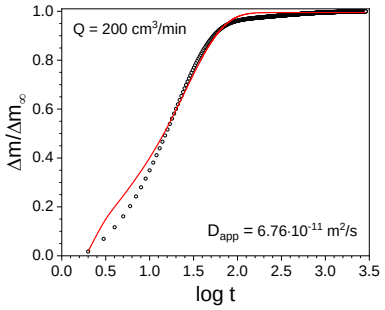

b)

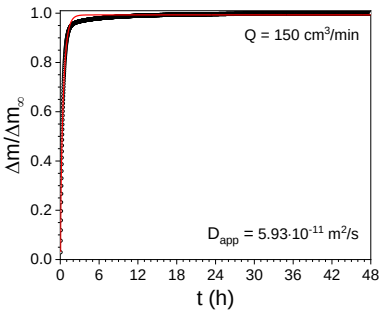

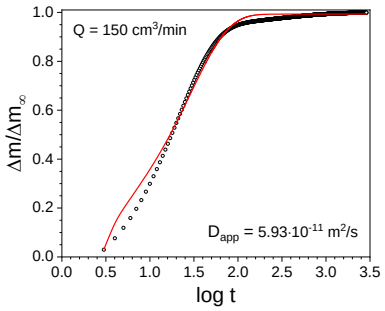

c)

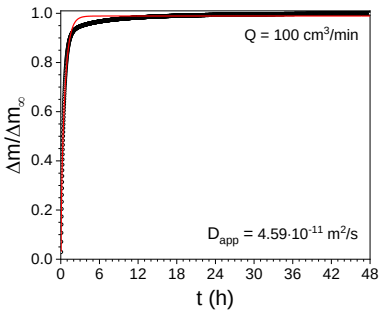

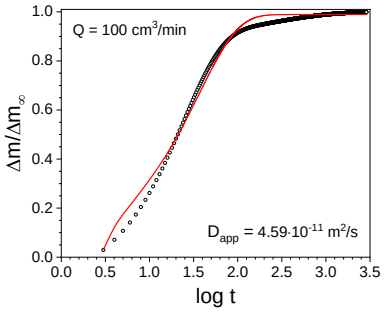

d)

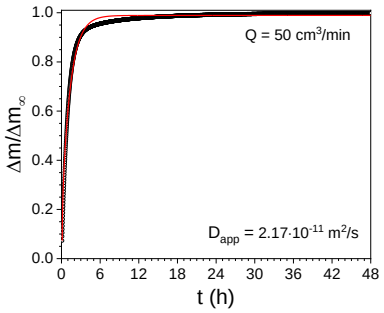

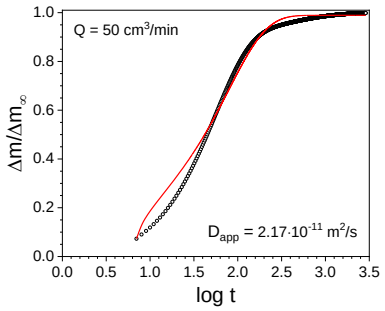

e)

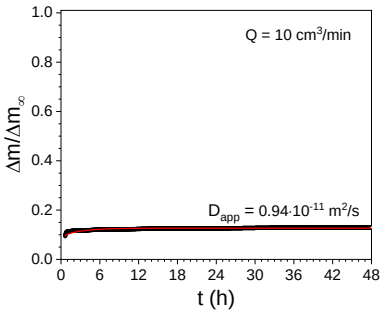

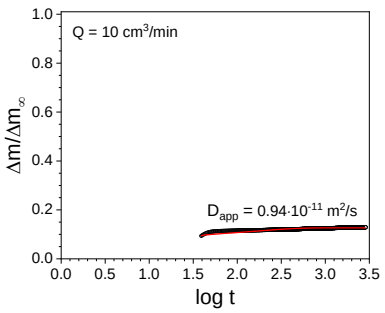

Fig. SI-7. lin-lin (left column) and lin-log (right column) plots of the time-sorption isotherm DVS data at different flow rate values Q for the spruce disk in the **L-direction**, together with the corresponding **SUM** fitting curve.

a)

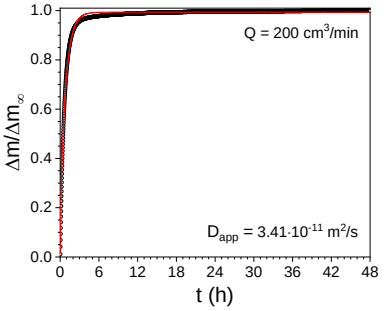

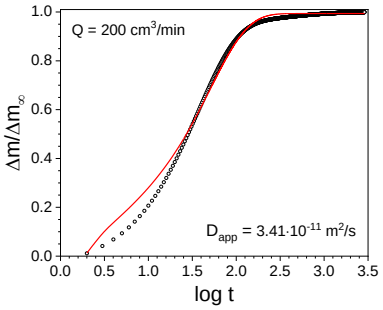

b)

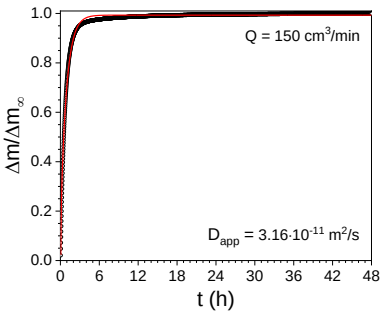

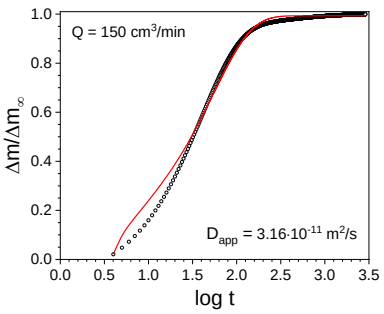

c)

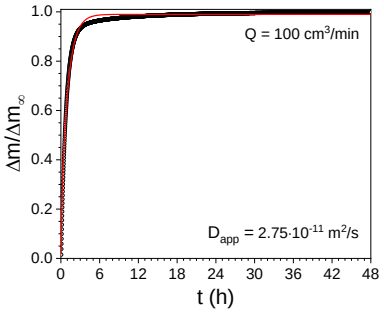

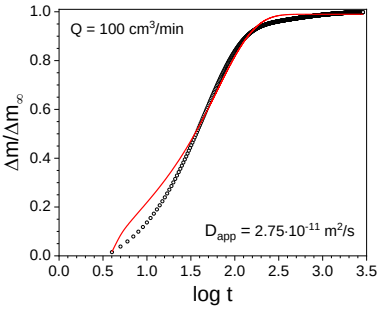

d)

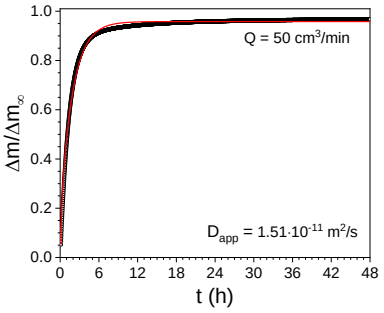

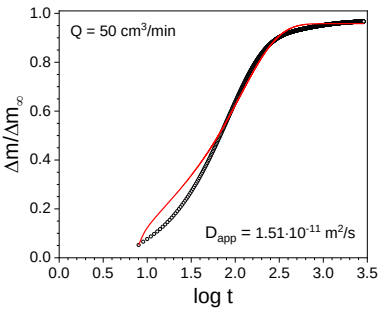

e)

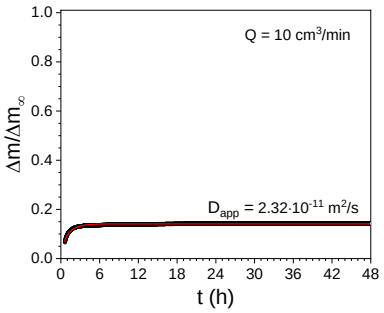

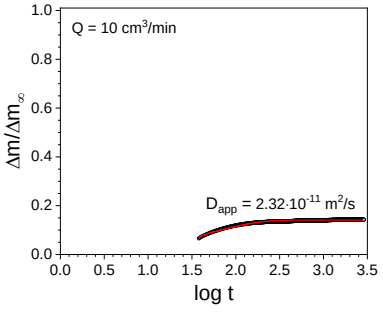

Fig. SI-8. lin-lin (left column) and lin-log (right column) plots of the time-sorption isotherm DVS data at different flow rate values Q for the spruce disk in the **R-direction**, together with the corresponding **SUM** fitting curve.

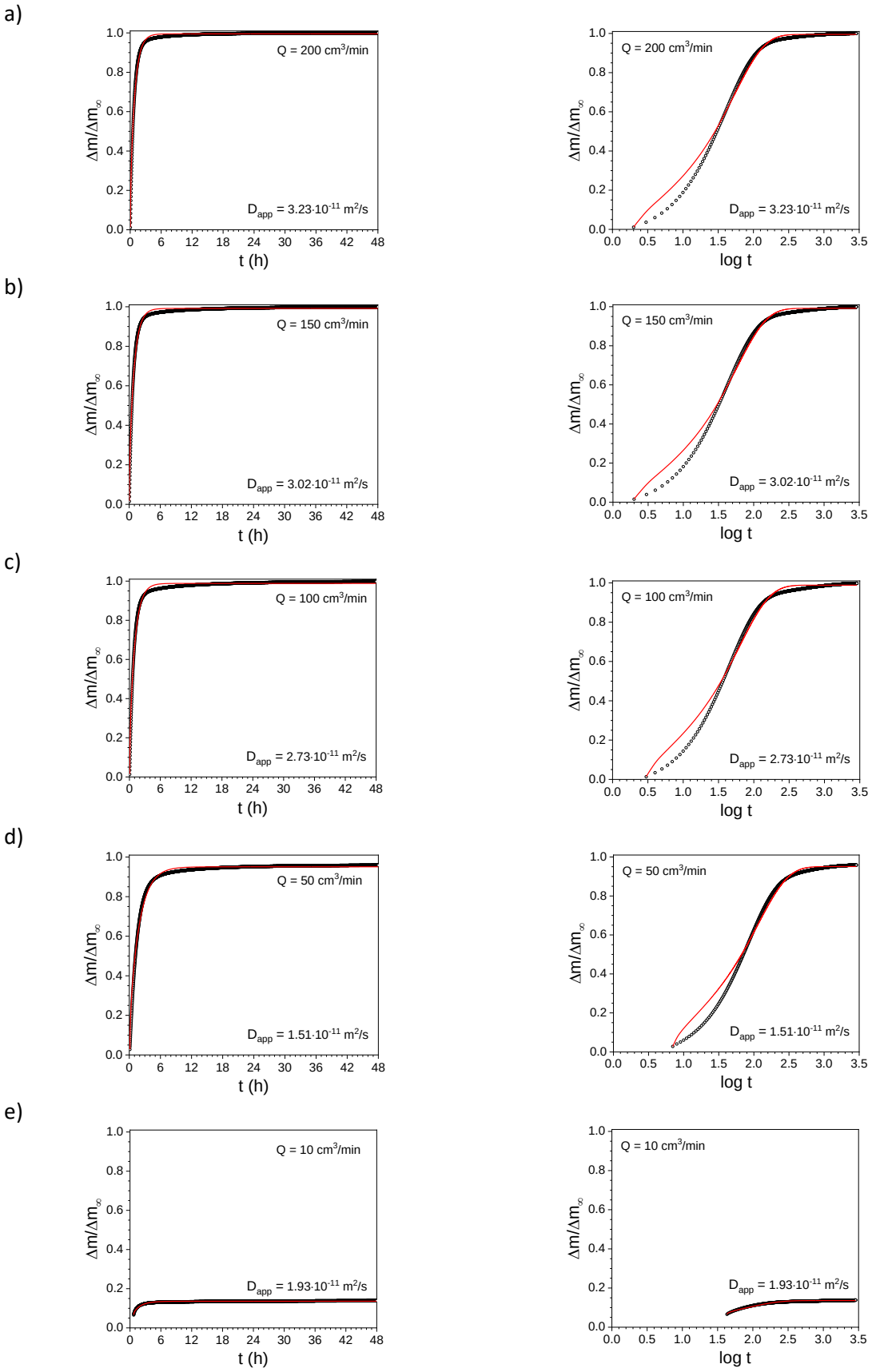

Fig. SI-9. lin-lin (left column) and lin-log (right column) plots of the time-sorption isotherm DVS data at different flow rate values Q for the spruce disk in the **T-direction**, together with the corresponding **SUM** fitting curve.

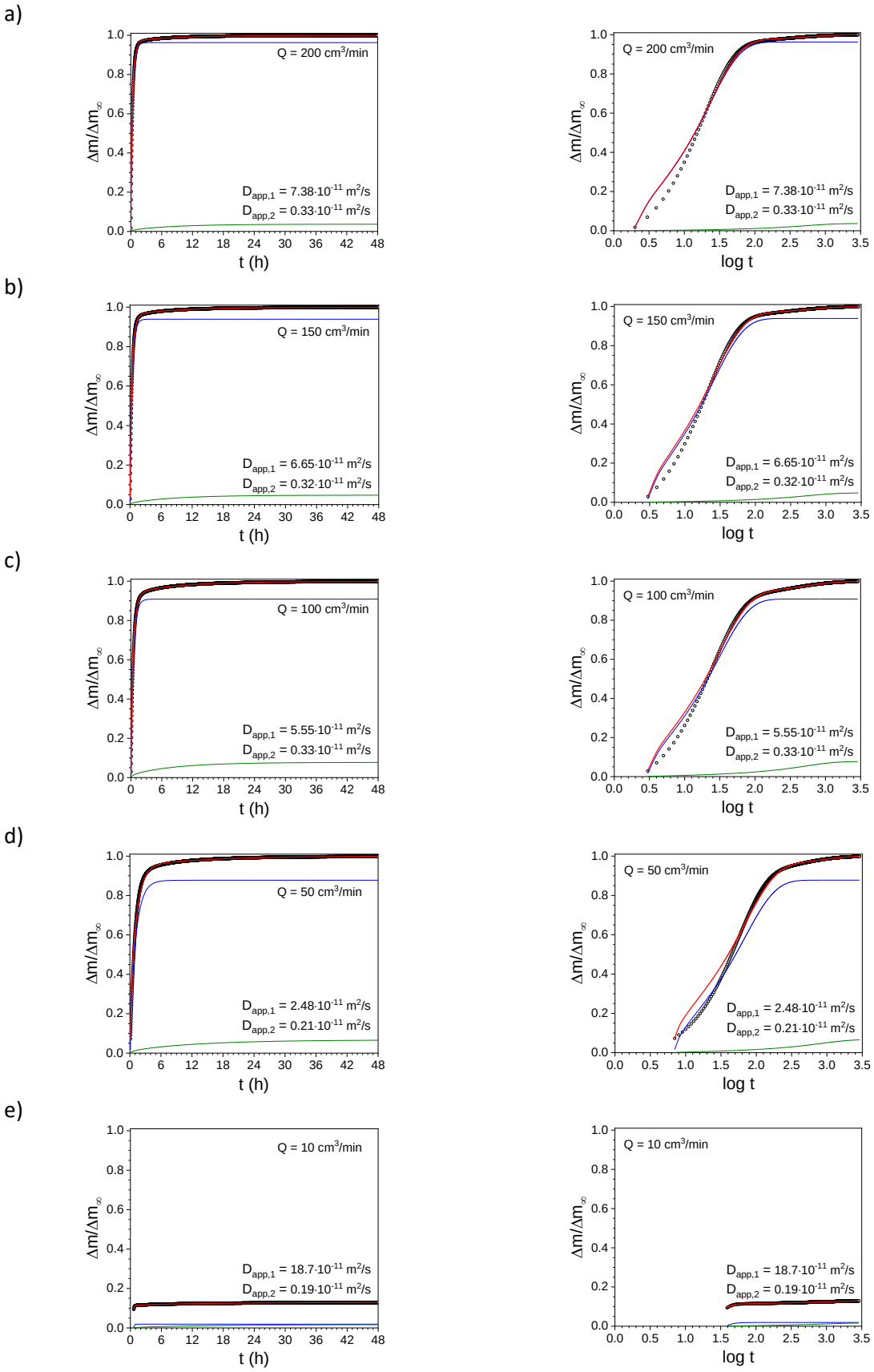

Fig. SI-10. lin-lin (left column) and lin-log (right column) plots of the time-sorption isotherm DVS data at different flow rate values Q for the spruce disk in the **L-direction**, together with the corresponding **DSUM** fitting curve.

a)

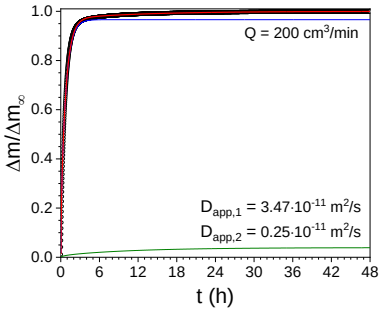

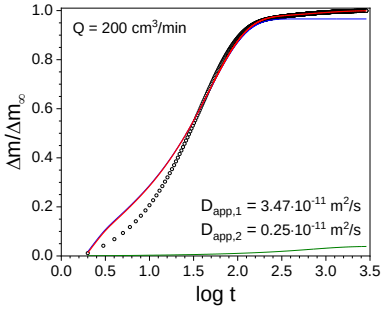

b)

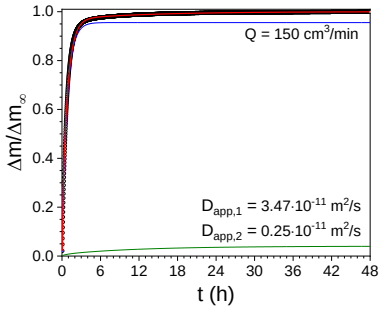

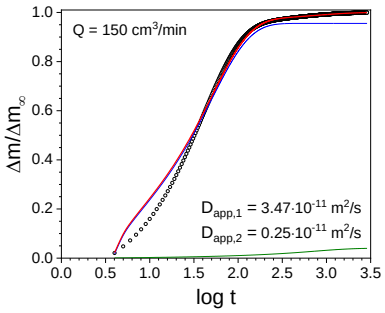

c)

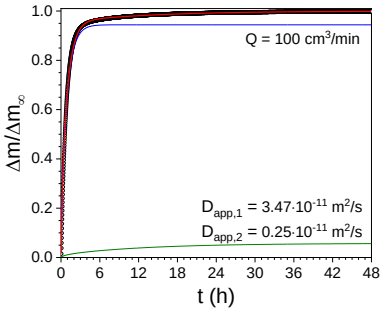

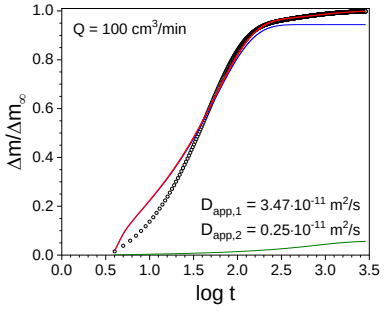

d)

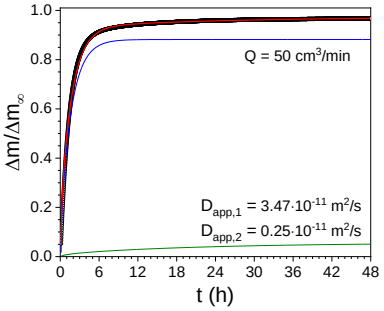

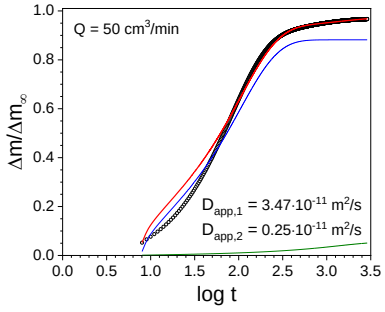

e)

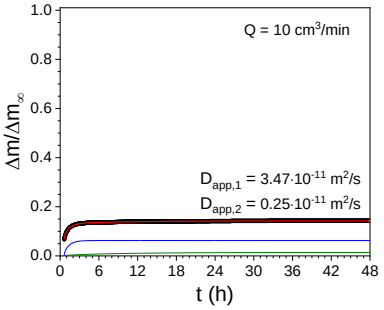

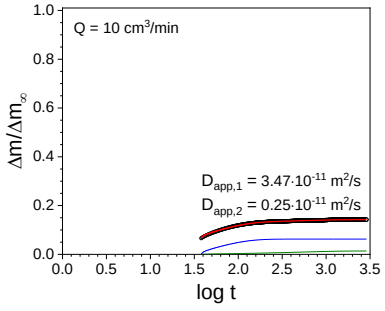

Fig. SI-11. lin-lin (left column) and lin-log (right column) plots of the time-sorption isotherm DVS data at different flow rate values Q for the spruce disk in the **R-direction**, together with the corresponding **DSUM** fitting curve.

a)

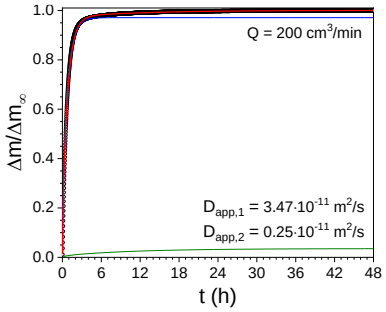

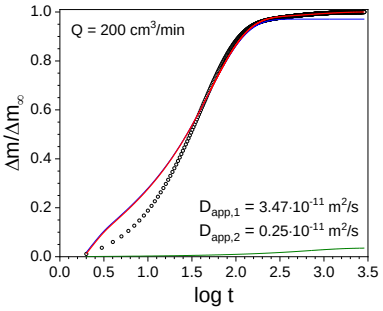

b)

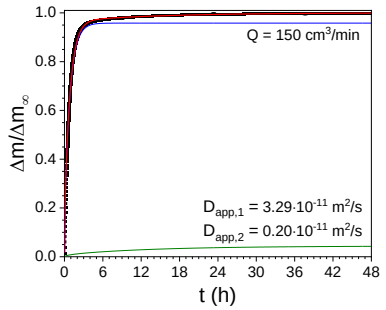

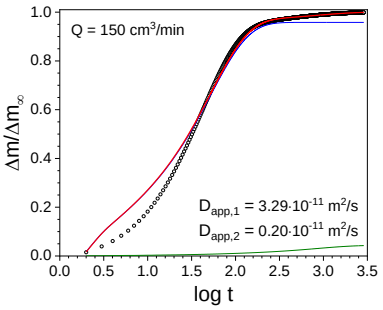

c)

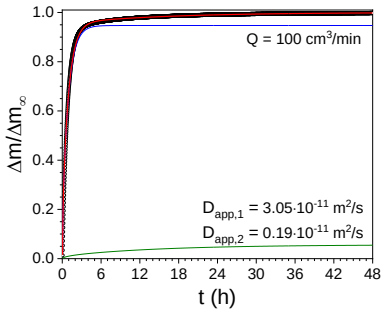

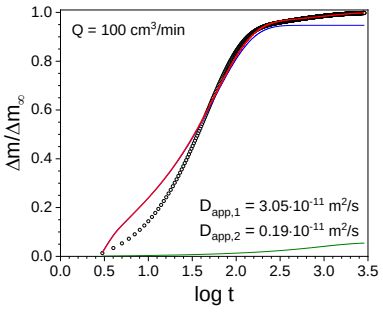

d)

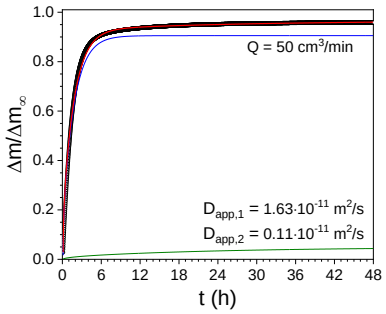

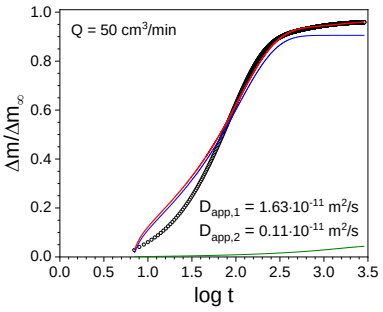

e)

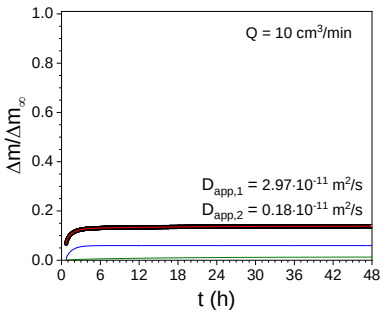

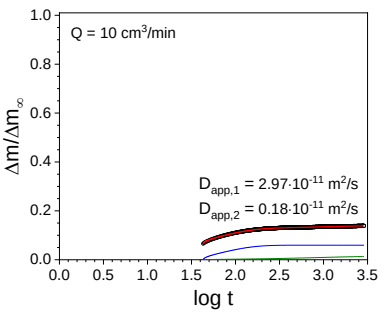

Fig. SI-12. lin-lin (left column) and lin-log (right column) plots of the time-sorption isotherm DVS data at different flow rate values Q for the spruce disk in the **T-direction**, together with the corresponding **DSUM** fitting curve.

Table SI-1. Time-sorption isotherm DSE fitting parameters and the apparent diffusion coefficient D_{DSE} at the different flow rate values Q for the spruce disk in the L-direction.

Q (cm^3/min)	A_1	A_2	τ_1 (min)	τ_2 (min)	β_1	β_2	τ (min)	β	D_{DSE} (10^{-10} m^2/s)
10	0.46±0.01	0.54±0.01	6.3±0.2	905±11	1.1±0.1	0.59±0.01	340±4	0.586±0.003	0.098±0.001
50	0.813±0.004	0.187±0.004	53.7±0.1	209±8	1.086±0.003	0.59±0.01	61±1	0.720±0.004	0.55±0.01
100	0.869±0.003	0.131±0.003	24.2±0.1	218±9	0.982±0.003	0.59±0.01	27.7±0.3	0.651±0.004	1.20±0.01
150	0.916±0.002	0.084±0.002	20.48±0.03	210±8	0.992±0.002	0.59±0.01	22.3±0.2	0.78±0.01	1.49±0.01
200	0.933±0.002	0.067±0.002	18.55±0.03	195±10	0.993±0.002	0.59±0.01	19.8±0.2	0.82±0.01	1.68±0.01

Table SI-2. Time-sorption isotherm DSE fitting parameters and the apparent diffusion coefficient D_{DSE} at the different flow rate values Q for the spruce disk in the R-direction.

Q (cm^3/min)	A_1	A_2	τ_1 (min)	τ_2 (min)	β_1	β_2	τ (min)	β	D_{DSE} (10^{-10} m^2/s)
10	0.87±0.01	0.13±0.01	37.4±0.3	611±18	0.85±0.01	1.15±0.03	51±1	0.586±0.003	0.65±0.01
50	0.821±0.002	0.179±0.002	79.7±0.1	260±6	1.046±0.002	0.60±0.01	89±1	0.760±0.004	0.371±0.003
100	0.889±0.002	0.111±0.002	43.41±0.04	289±9	1.004±0.002	0.63±0.01	48.2±0.4	0.756±0.004	0.69±0.01
150	0.910±0.003	0.090±0.003	39.33±0.04	230±12	0.985±0.002	0.60±0.01	42.5±0.3	0.80±0.01	0.78±0.01
200	0.912±0.003	0.088±0.003	36.49±0.04	210±13	0.976±0.002	0.59±0.01	39.3±0.3	0.80±0.01	0.84±0.01

Table SI-3. Time-sorption isotherm DSE fitting parameters and the apparent diffusion coefficient D_{DSE} at the different flow rate values Q for the spruce disk in the T-direction

Q (cm^3/min)	A_1	A_2	τ_1 (min)	τ_2 (min)	β_1	β_2	τ (min)	β	D_{DSE} (10^{-10} m^2/s)
10	0.872±0.002	0.128±0.002	45.9±0.2	1106±11	0.779±0.003	1.15±0.01	66±1	0.586±0.003	0.57±0.01
50	0.810±0.002	0.190±0.002	81.1±0.1	228±5	1.097±0.002	0.61±0.01	90±1	0.795±0.005	0.426±0.003
100	0.883±0.002	0.117±0.002	44.31±0.03	290±9	1.042±0.002	0.59±0.01	49.1±0.4	0.768±0.004	0.78±0.01
150	0.903±0.002	0.097±0.002	41.28±0.03	291±9	1.010±0.001	0.59±0.01	43.4±0.4	0.80±0.01	0.88±0.01
200	0.911±0.002	0.089±0.002	38.75±0.02	200±7	1.006±0.001	0.64±0.01	41.7±0.3	0.83±0.01	0.91±0.01

Table SI-4. Time-sorption isotherm RP fitting parameters and the apparent diffusion coefficient D_{RP} at the different flow rate values Q for the spruce disk in the L-, R- and T-direction.

Q (cm^3/min)	τ (L) (min)	τ (R) (min)	τ (T) (min)	n (L)	n (R)	n (T)	D_{RP} (L) (10^{-10} m^2/s)	D_{RP} (R) (10^{-10} m^2/s)	D_{RP} (T) (10^{-10} m^2/s)
50	100±0	145±1	143±1	0.857±0.001	0.842±0.005	0.867±0.005	0.333±0.001	0.227±0.002	0.267±0.002
100	37±1	66±1	67±1	0.916±0.011	0.908±0.012	0.922±0.011	0.893±0.015	0.505±0.009	0.569±0.009
150	31±1	60±1	60±1	0.914±0.012	0.881±0.012	0.880±0.012	1.078±0.020	0.554±0.011	0.632±0.012
200	27±1	54±1	59±1	0.925±0.015	0.885±0.014	0.883±0.012	1.236±0.026	0.615±0.014	0.651±0.013

Table SI-5. The apparent diffusion coefficient D_{SUM} at the different flow rate values Q for the spruce disk in the L-, R and T-direction.

Q (cm^3/min)	D_{SUM} (L) (10^{-10} m^2/s)	D_{SUM} (R) (10^{-10} m^2/s)	D_{SUM} (T) (10^{-10} m^2/s)
10	0.094	0.232	0.193
50	0.217	0.151	0.151
100	0.459	0.275	0.273
150	0.593	0.316	0.302
200	0.676	0.341	0.323

Table SI-6. Time-sorption isotherm DSUM fitting parameters and the apparent diffusion coefficient D_{DSUM} at the different flow rate values Q for the spruce disk in the L-direction.

Q (cm^3/min)	A_1	A_2	D_1 (10^{-10} m^2/s)	D_2 (10^{-10} m^2/s)	D_{DSUM} (10^{-10} m^2/s)
10	0.534	0.466	1.87	0.019	0.059
50	0.929	0.071	0.248	0.021	0.225
100	0.922	0.078	0.555	0.033	0.495
150	0.952	0.048	0.665	0.032	0.621
200	0.963	0.037	0.738	0.033	0.702

Table SI-7. Time-sorption isotherm DSUM fitting parameters and the apparent diffusion coefficient D_{DSUM} at the different flow rate values Q for the spruce disk in the R-direction.

Q (cm^3/min)	A_1	A_2	D_1 (10^{-10} m^2/s)	D_2 (10^{-10} m^2/s)	D_{DSUM} (10^{-10} m^2/s)
10	0.818	0.182	0.362	0.031	0.255
50	0.940	0.060	0.166	0.013	0.152
100	0.943	0.057	0.309	0.022	0.285
150	0.959	0.041	0.343	0.023	0.325
200	0.961	0.039	0.370	0.025	0.351

Table SI-8. Time-sorption isotherm DSUM fitting parameters and the apparent diffusion coefficient D_{DSUM} at the different flow rate values Q for the spruce disk in the T-direction

Q (cm^3/min)	A_1	A_2	D_1 (10^{-10} m^2/s)	D_2 (10^{-10} m^2/s)	D_{DSUM} (10^{-10} m^2/s)
10	0.815	0.185	0.297	0.018	0.198
50	0.948	0.052	0.163	0.011	0.152
100	0.944	0.056	0.305	0.019	0.282
150	0.956	0.044	0.329	0.020	0.310
200	0.965	0.035	0.347	0.025	0.331

Table SI-9. Apparent diffusion coefficient $D_{0.63}$ calculated from the lifetime value $t_{0.63}$ at the different flow rate values Q for the spruce disk in the L-, R- and T-direction.

Q (cm^3/min)	$t_{0.63}$ (L) (min)	$t_{0.63}$ (R) (min)	$t_{0.63}$ (T) (min)	$D_{0.63}$ (L) (10^{-10} m^2/s)	$D_{0.63}$ (R) (10^{-10} m^2/s)	$D_{0.63}$ (T) (10^{-10} m^2/s)
50	64	98	101	1.59	0.814	0.776
100	30	52	52	1.39	0.726	0.726
150	24	46	46	1.11	0.642	0.642
200	21	41	43	0.522	0.341	0.331

Table SI-10. Apparent diffusion coefficient $D_{0.5}$ calculated from the half-life time value $t_{0.5}$ at the different flow rate values Q for the spruce disk in the L-, R- and T-direction.

Q (cm^3/min)	$t_{0.5}$ (L) (min)	$t_{0.5}$ (R) (min)	$t_{0.5}$ (T) (min)	$D_{0.5}$ (L) (10^{-10} m^2/s)	$D_{0.5}$ (R) (10^{-10} m^2/s)	$D_{0.5}$ (T) (10^{-10} m^2/s)
50	44	67	71	0.189	0.124	0.117
100	20	36	36	0.417	0.231	0.231
150	17	32	32	0.490	0.260	0.260
200	15	28	30	0.555	0.298	0.278

Table SI-11. Apparent diffusion coefficient D_{app} calculated from the time at the local maximum t_{max} from the DER method at the different flow rate values Q for the spruce disk in the L-, R- and T-direction.

Q (cm^3/min)	t_{max} (L) (min)	t_{max} (R) (min)	t_{max} (T) (min)	D_{DER} (L) (10^{-10} m^2/s)	D_{DER} (R) (10^{-10} m^2/s)	D_{DER} (T) (10^{-10} m^2/s)
50	52.5	79.7	82.1	0.636	0.415	0.465
100	20.8	40.0	43.3	1.603	0.826	0.882
150	18.2	37.0	39.5	1.830	0.894	0.967
200	16.4	34.4	37.8	2.041	0.961	1.009

Table SI-12. Shape factor β calculated from the peak's FWHM from the DER method at the different flow rate values Q for the spruce disk in the L-, R- and T-direction.

Q (cm^3/min)	FWHM (L)	FWHM (R)	FWHM	β (L)	β (R)	β (T)
50	0.926	1.055	1.007	1.147	1.007	1.054
100	1.024	1.095	1.057	1.038	0.970	1.005
150	1.017	1.123	1.101	1.045	0.946	0.965
200	1.036	1.131	1.109	1.025	0.939	0.958

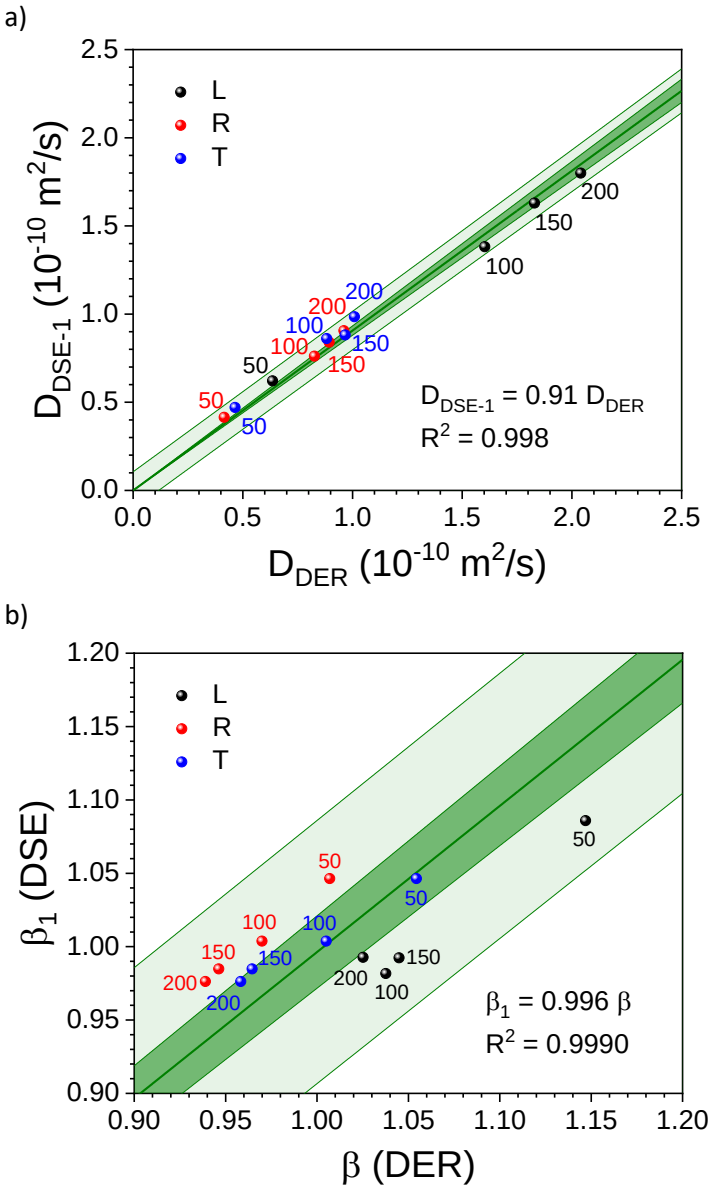

Fig. SI-13. a) Linear relationship between the apparent diffusion coefficient D_{DSE-1} from the DSE fitting model and the shape factor β from the DER method for the three wood directions, *i.e.*, L, R and T, and flow rate Q values. b) Linear relationship between the shape factor β_1 from the DSE fitting model and the shape factor β from the DER method for the three wood directions, *i.e.*, L, R and T, and flow rate Q values. Note: 95% confidence band (deep green), 95% prediction band (light green)

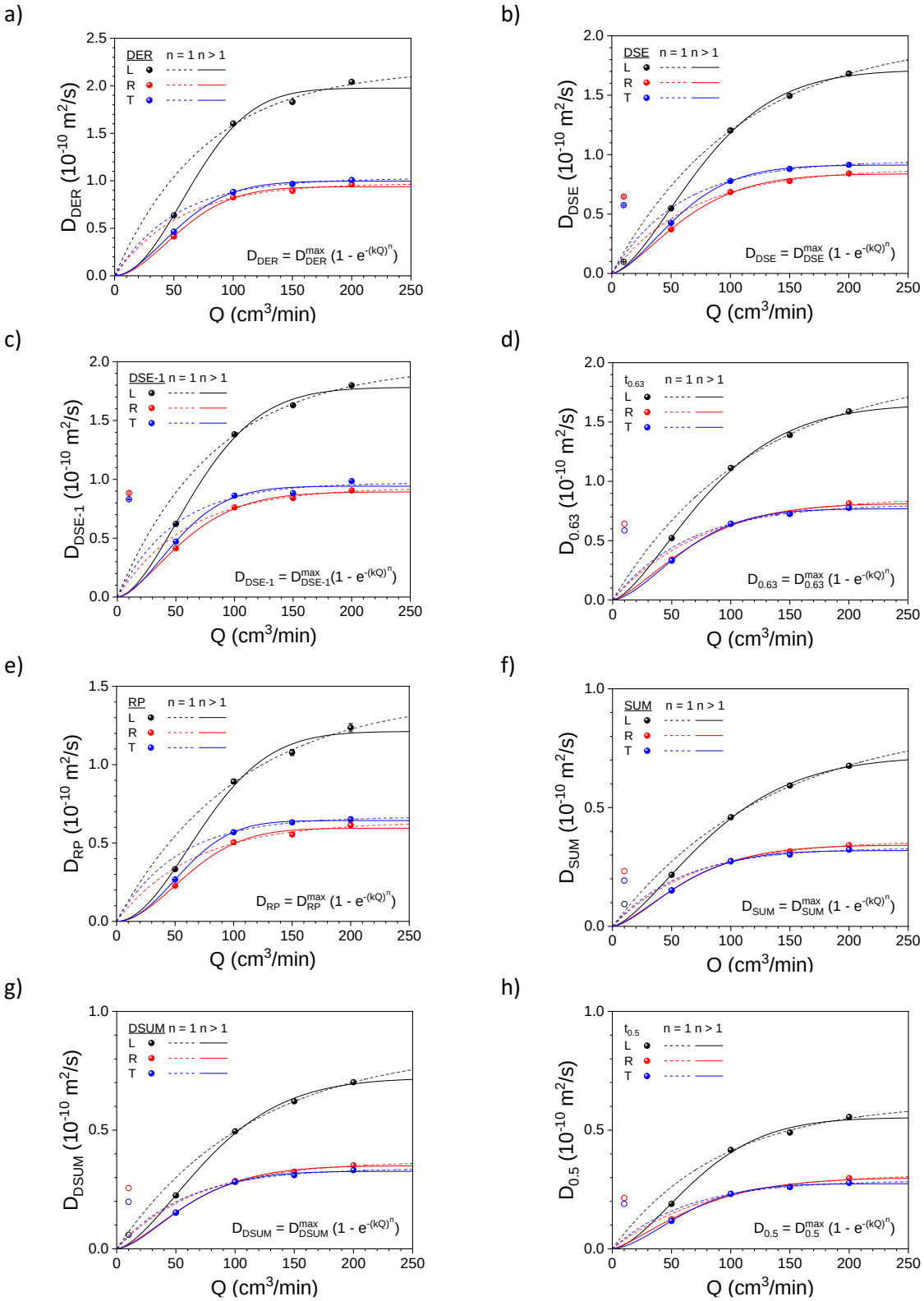

Fig. SI-14. Apparent diffusion coefficient (D_{app}) values from 30% to 80% RH as a function of the flow rate (Q) for the three wood directions, *i.e.*, L, R and T, obtained from of the experimental data in Figure 1 using the different fitting models and approaches, *i.e.*, a) the derivative method (DER), b) the double-stretched exponential function (DSE), c) the fast sorption process in the double-stretched exponential function (DSE-1), c) the lifetime value ($t_{0.63}$), d) the Ritger-Peppas function (RP), e) the Fickian function (SUM), f) the double-Fickian function (DSUM), and g) the half-life time value ($t_{0.5}$). The curves correspond to the data in the three wood directions, following an exponential function (n = 1, dashed lines) and a stretched exponential function (n > 1, solid lines).

Table SI-13. Flow rate constant k and maximum apparent diffusion coefficient D_{app}^{max} from the fitting (n = 1) of the apparent diffusion coefficient D_{app} at different flow rate values Q obtained from the derivative method (DER), the double-stretched exponential function (DSE), the fast sorption process in the double-stretched exponential function (DSE-1), the lifetime value ($t_{0.63}$), the Ritger-Peppas function (RP), the Fickian function (SUM), the double-Fickian function (DSUM), and the half-life time value ($t_{0.5}$) for the spruce disk in the L-, R- and T-direction.

	L		R		T	
	k (10^{-3} min/cm³)	D_{app}^{max} (10^{-10} cm³/min	k (10^{-3} min/cm³)	D_{app}^{max} (10^{-10} cm³/min	k (10^{-3} min/cm³)	D_{app}^{max} (10^{-10} cm³/min
DER	13±2	2.18±0.04	19±3	0.97±0.03	20±1	1.03±0.01
DSE	9.2±0.1	2.00±0.01	15±1	0.88±0.02	17±1	0.95±0.01
DSE-1	12±1	1.97±0.04	12±2	0.93±0.03	21±8	0.97±0.04
$t_{0.63}$	8.5±0.3	1.94±0.03	13±2	0.86±0.04	16±1	0.81±0.01
RP	10±1	1.44±0.04	15±3	0.63±0.04	19±1	0.67±0.01
SUM	7.5±0.3	0.87±0.02	14±1	0.36±0.01	17±2	0.33±0.01
DSUM	8.7±0.1	0.85±0.00	15±1	0.37±0.01	18±2	0.34±0.01
$t_{0.5}$	11±1	0.62±0.03	13±3	0.32±0.03	16±1	0.29±0.01

Table SI-14. Flow rate constant k and maximum apparent diffusion coefficient D_{app}^{max} from the fitting (n > 1) of the apparent diffusion coefficient D_{app} at different flow rate values Q obtained from the derivative method (DER), the double-stretched exponential function (DSE), the fast sorption process in the double-stretched exponential function (DSE-1), the lifetime value ($t_{0.63}$), the Ritger-Peppas function (RP), the Fickian function (SUM), the double-Fickian function (DSUM), and the half-life time value ($t_{0.5}$) for the spruce disk in the L-, R- and T-direction.

	L		R		T	
	k (10^{-3} min/cm³)	D_{app}^{max} (10^{-10} cm³/min	k (10^{-3} min/cm³)	D_{app}^{max} (10^{-10} cm³/min	k (10^{-3} min/cm³)	D_{app}^{max} (10^{-10} cm³/min
DER	12.5±0.4	1.98±0.04	14.9±0.4	0.94±0.02	15.4±0.3	1.00±0.01
DSE	11.0±0.4	1.71±0.04	14.0±0.4	0.84±0.02	14.9±0.2	0.91±0.01
DSE-1	12.3±0.4	1.78±0.04	12.3±0.4	0.89±0.02	16.2±0.4	0.94±0.03
$t_{0.63}$	10.5±0.4	1.65±0.04	13.1±0.4	0.81±0.03	14.1±0.4	0.77±0.01
RP	11.2±0.4	1.21±0.04	13.6±0.4	0.59±0.02	14.7±0.2	0.64±0.01
SUM	10.0±0.2	0.72±0.01	13.8±0.4	0.34±0.01	15.0±0.4	0.32±0.01
DSUM	10.8±0.3	0.72±0.01	13.8±0.4	0.35±0.01	15.0±0.4	0.33±0.01
$t_{0.5}$	11.8±0.4	0.55±0.02	12.7±0.4	0.30±0.01	14.2±0.4	0.27±0.01